Pyrolysis of ficus nitida wood: Determination of kinetic and thermodynamic parameters

A. Tabal, Abdellatif Barakat, A. Aboulkas, K. El Harfi

Pyrolysis of ficus nitida wood: Determination of kinetic and thermodynamic parameters

A. Tabal [a], A. Barakat [b,c], A. Aboulkas [a*], K. El harfi [a**]

[a] Laboratoire des procédés chimiques et matériaux appliqués (LPCMA), Faculté polydisciplinaire de Béni-Mellal, Université Sultan Moulay Slimane, BP 592, 23000 Béni-Mellal, Morocco.

[b] IATE, Montpellier University, INRAE, Agro Institut, 2, Place Pierre Viala, 34060 Montpellier, France.

[c] Mohammed VI Polytechnic University, Lot 660, Hay Moulay Rachid, 43150 Ben Guerir, Morocco.

E-mail address: * a.aboulkas@usms.ma (A. Aboulkas)
                          ** elharfi@yahoo.fr (K. El harfi)

Abstract:

In the present work, the kinetic and thermodynamic analysis of ficus wood was carried out using the thermogravimetric analysis (TGA). Thermal degradation of ficus wood has been evaluated under dynamic conditions from 373 K to 1173 K at heating rates of 5, 10, 20, and 50 K.min^{-1}. The kinetic analysis was performed using isoconversional methods (Friedman (FR), Flynn-Wall-Ozawa (FWO) and Vyazovkin (VYA)) and the integral master-plots method to estimate the kinetic triplets. The thermogravimetric and kinetic data were used to calculate the thermodynamic parameters (ΔG, ΔH and ΔS) and kinetic compensation effects. The conversion range of $0.05 \leq x \leq 0.9$ shows clearly that the pyrolysis of ficus wood could represent a triple-step reaction, which corresponds to the pyrolysis of hemicellulose, cellulose, and lignin, respectively. From the isoconversional plots of ficus wood having average activation energy values of 171.4-180.3 kJ.mol^{-1}, 206.48-214.42 kJ.mol^{-1} and 237.85-248.23 kJ.mol^{-1} for hemicellulose, hemicellulose, and lignin, respectively. The experimental data of focus wood had overlapped the D4, D2, and F3 in the conversion range of 5-35%, 35-75%, and 75-90%, respectively. All values of ΔH and ΔG maintain at a positive constant, whereas

the value of ΔS is negative in the range of 5-35%. The difference between E-values and the ΔH value for the three pseudo-components of ficus wood is about ≈ 5 kJ.mol^{-1}. The kinetic and thermodynamic parameters will be beneficial in assimilating the thermal decomposition of ficus wood for its use in bioenergy.

1-Introduction:

In the context of the depletion of fossil fuel resources and the reduction of climatic risks as linked to greenhouse gas emissions, the interest in renewable energies appears as an attention to the development and improvement of alternative energy sources which contributes to respond the current global environmental concern and the global energy needs [1,2]. Among all renewable alternatives, the energy obtained from biomass, represent a renewable alternative with a high potential. The biomass has attracted a great attention as a source for clean energy, environmental-friendly and CO_2 neutral energy source. Lignocellulosic biomass, otherwise known as second generation biomass, has great potential in comparison with sugar and starchy plants or other fossil hydrocarbons, offers better energy and environmental balances (reduction in water and fertilizer consumption)[3,4].

In recent years, the utilization of dedicated energy crops has been a significant potential for bio-energy application[5,6]. The wood cultivated has proved to be an interesting resource. The conversion of wood biomass results in biofuels called second-generation biofuels. These wood biomass can be converted directly into liquid, gaseous and solid fuels, usable for transport, heat and/or power production [7–9].

Morocco has a large forest area which ensures it a large annual production of wood biomass which is used for different purposes (lumber, fuel wood, production of charcoal, production of pulp, etc.)[10–12]. In recent years, the ficus nitida tree has known a great diffusion in morocco, in the green zones, in the boulevards, in the river and public garden ... etc. It can be grown under harsh conditions where there is a little water and effort. This tree can be used for the environmental considerations and can be used as a dedicated energy culture. However, its exploitation in the world and in Morocco in particular is still very wrong organized. In this sense, research on the wood biomass valorization is numerous and is continuously growing, in order to optimize its exploitation and that of its waste[13,14].

Among the diver's valorization, thermochemical processes appear to be one of the main alternatives. The environmental benefits of thermochemistry are the reduction in the mass and volume of solids removed, the reduction of pollutants and the potential for pollution and the potential for energy recovery [15–17]. The pyrolysis is one of the promising technologies for converting biomass into high-value-added chemicals and biofuels. Depending on the operating conditions (such as temperature, heating rate, residence time, size of particles, moisture, pressure and nature of biomass material), the biomass can be converted into bio-oil, bio-gas and bio-char [18–21].

To understand the pyrolysis reaction, the knowledge of the pyrolysis kinetic characteristics and thermodynamic parameters are very important to study the thermal decomposition of biomass and determine their possible valorization process and it is imperative for the design and optimization of reactors [22–27]. Thermogravimetric analysis is the most common technique used to estimate the kinetic triplets and thermodynamic parameters of pyrolysis process. Several studies have focused on the kinetic parameters of wood decomposition [22,28–32]. Slopiecka et al. [22] investigated the poplar wood pyrolysis using a thermogravimetric study. The authors divided the pyrolysis process of wood into three

stages as material drying, passive and active pyrolysis. The results show that the average activation energy values are 153.92, 158.58 and 157.27 kJ mol^{-1} from the Kissinger, FWO and KAS models, respectively. M. Poletto [30] calculated the E values using FWO method to use them to determine the decomposition mechanisms. The results also showed that the degradation mechanism for both woods is governed by diffusion process, mainly by diffusion process in three dimensions, a D3 mechanism. The devolatilization behavior of several hardwoods and softwoods grown in Europe and USA, was investigated by Grønli et al. [28] using thermogravimetric analyzer to temperature of to 723 K with heating rate of 5 K/min. The authors show that the decomposition of all wood is as one reaction. The authors show that decomposition of all wood is mainly occurred as three parallel reactions. The average activation energies are 100, 236, and 46 kJ/mol for hemicellulose, cellulose, and lignin, respectively. Mishra et al. [29] presented a kinetics of pinewood decomposition. The results show that the decomposition mechanism is observed to be governed by a diffusion mechanism up to conversion values of 0.7 and then by a 1½ order reaction. The authors state that the decomposition mechanism obeys of 2D diffusion. The isoconversional plots show three stages with activation energy values of 134.32, 146.89 and 155.76 kJ/mol, respectively.

The model-free isoconversional methods showed a clear dependence of activation energy on the reaction extent, suggesting that the pyrolysis process includes many different reactions occurring at the same time. The pyrolysis process of biomass may be considered as a pseudo-components approach, separating the individual processes by derivative TGA (DTG) peak followed by the kinetic, mechanistic and thermodynamic modeling of the resulting individual curves. Few studies have been reported for kinetic, mechanistic and thermodynamic analysis of biomass pyrolysis using the pseudo-components approach. In particular, ficus nitida wood kinetic, mechanistic and thermodynamic analysis using this approach has not been reported yet.

According to this, the objective of this research is to quantitatively identify the thermal decomposition characteristics of ficus nitida wood. Firstly, the TGA experiments of ficus wood were performed using a thermogravimetric analyzer with four different heating rates, e.g. 5, 10, 20, and 50 C.min^{-1}. Secondly, based on the TGA results, the isoconversional methods combined with the master-plots integral method is used to determine the activation energies and reaction models g(α) during the pyrolysis process of ficus wood. Finally, with the obtained activation energies, the thermodynamic parameters including pre-exponential factor (A) in Arrhenius equation, as well as the changes of enthalpy (ΔH), free Gibbs energy (ΔG), and entropy (ΔS) were also calculated.

2-Experimental techniques

2.1. Materials

The biomass sample used in this study was ficus nitida wood extracted from one trunk. This trunk was harvested in the green zones in region of Beni Mellal-Khenifra (Morocco). The sample was milled and sieved to a size range of 0.1 to 0.2 mm. Moisture percentage, Ash percentage and Volatile matter were determined using thermogravimetric analysis.

Fixed carbon was calculated by:

$$\textbf{Fixed carbon (wt\%)} = \textbf{100} - (\textbf{Ash (wt\%)} + \textbf{Volatile Matter(wt\%)})$$

To give an overview of the properties of the raw material, the immediate, final and biochemical composition of ficus nitida wood was carried out, and the results are listed in Table 1.

2.2. Pyrolysis Experiment

Ficus nitida wood samples were subjected to thermogravimetric analysis (TGA) in nitrogen atmosphere. SETARAM- LABSYS evo STA 1600 analyzer was used to measure and record the change in sample mass with temperature during the pyrolysis reaction. The thermogravimetric experiments were conducted in nitrogen atmosphere from 373 k and 1173 K at four heating rates of 5, 10, 20, and 50 K/min. The flow rate of high purity nitrogen was 60 mL.min^{-1}. The experiments were carried out two or three times for the accuracy of results.

2.3. Kinetic theory

In the kinetic, thermal decomposition results from the reactions of solid / gas systems which obey the following reaction scheme:

Biomass (Solid) → Volatile (gases + tar) + Char (solid residue)

For non-isothermal decomposition experiments, the rate of heterogeneous solid-state reactions can be generally described by

$$\frac{dx}{dt} = k(T)f(x) \qquad (1)$$

x is the conversion; T is the temperature; K (T) is a temperature-dependent constant; f(x) is the reaction model.

According to Arrheniuss equation, the rate constant was

$$k(T) = A \, exp\left(\frac{-E}{RT}\right) \qquad (2)$$

k(T) is the rate constant; E is the apparent activation energy; A is the frequency factor; f(x) is the reaction model; R is the gas constant.

By combining the Eqs. (1) and (2), the reaction rate can be written in the form:

$$\frac{dx}{dt} = A. exp\left(\frac{-E}{RT}\right)f(x) \qquad (3)$$

Integrating the equation (3) for a constant rate of heating β, it became:

$$g(x) = \int_0^x \frac{dx}{f(x)} = \frac{A}{\beta} \int_{T0}^T exp\left(-\frac{E}{RT}\right) dT = \frac{AE}{\beta R} p(u) \qquad (4)$$

where g(α) is the integral form of the conversion dependence function f(x) (Table 2). This Eq. (4) has no explicit solution.

2.3.1. Determination of activation energy

2.3.1.1 Differential isoconversional method of Friedman.

This method is a differential isoconversional method and probably the most general, since it is a direct integration of the equation (3) after having carried its logarithm, which gives [33]:

$$ln\left(\frac{dx}{dt}\right) = ln[Af(x)] - \left(\frac{E}{RT}\right) \qquad (5)$$

The apparent activation energy could be determined by plotting $ln\left(\frac{dx}{dt}\right)$ against 1/T under a given value of x.

2.3.1.2 Integral isoconversional method of Flynn–Wall–Ozawa method (FWO).

All the integral isoconversional methods are established on the different assumptions of p(u) in Eq. (4). Flynn-Wall-Ozawa (FWO) method [34–36], uses the Doyle's approximation of p(x) [37], and can determine the Ea values without any knowledge of the reaction mechanisms.

$$ln(\beta) = ln\left(\frac{AE}{Rg(x)}\right) - 5,331 - 1,052\frac{E}{RT} \qquad (6)$$

Thus, for each value of x, E is calculated from the slope of the plot $ln(\beta)$ versus 1/T in Eq. (6).

2.3.1.3 Integral isoconversional method of Vyazovkin (VYA)

The Vyazovkin method [38,39] is based on the following expression:

$$\ln\left(\frac{\beta}{T^2}\right) = \ln\left(\frac{AR}{Eg(x)}\right) - \frac{E}{RT} \qquad (7)$$

The apparent activation energy can be calculated from the plot of $\ln(\beta/T^2)$ as a function $1/T$ for each value of x, where the slope is $= - E/R$.

2.3.2 Prediction of reaction model using master plots method

The master plots method can be used to predict the reaction mechanism that describes the pyrolysis of ficus nitida wood. This method uses the eq (4):

$$g(x) = \frac{AE}{\beta R}p(u) \qquad (8)$$

Where p(u) defined as:

$$p(u) = \int_{\infty}^{u} -\left(\frac{e^{-u}}{u^2}\right)du \qquad (9)$$

where u = E/RT.

Doyle's approximation [40] can be used to obtain of equation solution of p(u). From Eq. (8) and taking x = 0.5 as a reference it follows:

$$g(0.5) = \frac{AE}{\beta R}p(u_{0.5}) \qquad (10)$$

The ratio of Eq. (8) and Eq. (10) yields;

$$\frac{g(x)}{g(0,5)} = \frac{P(u)}{P(u_{0,5})} \qquad (11)$$

The term $\frac{P(u)}{P(u_{0,5})} = \frac{T^2}{T^2_{0,5}} \frac{exp(-E/RT)}{exp(-E/RT_{0,5})}$ is used to represent the experimental curves for each

heating rate. By comparing these experimental curves with the curves $\frac{g(x)}{g(0,5)}$ for each model,

the type of mechanism involved in the thermal degradation can be identified.

2.4. Determination of pre-exponential factor and thermodynamic parameter

Thermodynamic consideration is important for understanding the variation of enthalpy ΔH, entropy ΔS, and free energy ΔG with conversion. The pre-exponential factor was calculated according to the Kissinger method (Eq. 12). This method is used at different heating rate; however, it gives only one activation energy value for the overall conversion process. It was therefore not used to determinate the activation energy in this study. When determining the activation energy at each conversion point, Eqs. (13) can be utilized to calculate pre-exponential factor.

$$ln\left(\frac{\beta}{T_m^2}\right) = ln\left(\frac{AR}{E}\right) - \frac{E}{RT_m} \qquad (12)$$

$$A = \frac{\beta E \, exp\left(\frac{E}{RT_m}\right)}{R \, T_m} \qquad (13)$$

Once the activation energy and pre-exponential factor was known at each conversion point, the three thermodynamic parameters of ΔH, ΔG, and ΔS can be calculated as the following expressions:

$$\Delta H° = E - RT \qquad (14)$$

$$\Delta G° = E + RT_m ln\left(\frac{K_B T_m}{hA}\right) \qquad (15)$$

$$\Delta S° = \frac{\Delta H° - \Delta G°}{T_m} \qquad (16)$$

where

T_m = Peak temperature of the DTG curve;

K_B = Boltzmann constant (1.381×10^{-23} J/K);

H = Plank constant (6.626×10^{-34} J.s)

3. Results and discussion

3.1. Characterization of raw material

The proximate analysis, ultimate analysis and fiber analysis are listed in Table 1. The results are presented as mass percentage (wt%). The proximate analysis shows that the sample had a volatile matter percentage of 69.8 w%, which indicates that the sample would produce condensable vapors during pyrolysis. The ash content of ficus nitida wood was 14.4 wt%. Higher content of ash may impart negative effect on the HHV. Inorganic minerals present in ash affects the mechanism of biomass pyrolysis.

From the ultimate analysis, the ficus nitida wood has a low carbon content (43.55 wt%), which indicated that the calorific value of the sample would be low. The HHV (16.82 MJ.kg^{-1}) is low due to the high ash content and low volatiles content of ficus nitida wood. The ultimate analysis shows also that the ficus wood had low nitrogen content (0.68 wt%). The wood with low nitrogen content can be good candidates for thermochemical conversion.

3.2. Thermal degradation process

The conversion x and derivative conversion x (dx/dt) curves of ficus nitida wood at four heating rates of 5, 10, 20 and 50 K.min^{-1} are shown in Fig. 1, respectively. Ficus nitida wood is a biomass, which contains cellulose, hemicellulose and lignin. Each pseudo-component has a different decomposition temperature region.

Three zones can be identified for thermal decomposition of ficus nitida wood from the conversion x curves. The first zone occurred in the temperature range from ambient to around 171-206 °C, is related to the moisture and some light volatiles. The main volatilization process occurs in the second zone which is also known as the active pyrolysis, ranging from 171-206 °C to about 447-475 °C. The third zone (mainly 447 °C - 900 °C) is probably attributed to the slow degradation of carbonaceous in the residues. It is note that two small peaks are induced in this zone. This reflects that the wood includes two important components which are reactive only when the temperature is higher than 447 °C. The last peak can be probably attributed to mineral components (metal carbonates). The second zone can be divided into three stages from dx/dt and d^2x/dt curves, which involves the main decomposition of hemicellulose, cellulose and lignin, respectively. In this zone, the large quantitie of volatiles is produced. By using second derivative method (Fig. 2), the initial temperature (T_i) and final temperature (T_f) of different stages are listed in Table 3. The first stage corresponds to the decomposition of hemicellulose which mainly occurred at 180-301 °C and that the second which corresponds to cellulose ranging from 301°C to 392 °C. Lignin, is a slow rate to decompose, can be seen in the third stage, as it has been decomposed in a temperature range from 180 to 574 °C. In general, the high peak of the dx/dt curve corresponds to the cellulose and the shoulder corresponds to the hemicellulose and lignin, which covers a wider range of temperature. As far as we know, for lignocellulosic biomass materials, the hemicellulose is usually associated with a shoulder in the DTG curve and the cellulose with the highest decomposition peak [41]. Chen et al. [42] found that temperature decomposition of hemicellulose, cellulose, and lignin for five lignocellulosic biomasses were 141-304 °C, 276-407 °C, and 380-588 °C at 10 °C/min, respectively. Kaur et al. [43] obtained that the main of active pyrolysis which involves the decomposition of hemicellulose, cellulose and of lignin at temperature range of 160-520 °C.

3.3. Determination of activation energy

Decomposition kinetics during the ficus nitida wood pyrolysis process were determined by using the isoconversionnal methods namely Friedman (Eq. (5)), Flynn-Wall-Ozawa (Eq. (6)) and Vyazovkin (Eq. (7)). The E values have been determined in a broad x interval of 10-90 % with an increment of not greater than 5% for the three stages.

Based on Eqs. (5), (6) and (7), for a specified x, the the apparent activation energy values can be calculated from the slope of the fitted straight line (-E/R). The isoconversional lines derived from the three methods for each component (hemicellulose, cellulose and lignin) within a selected conversion range of 0.1-0.9 are shown in Figs 3a, 4a and 5a, respectively. Table 4 summarizes the activation energy values and the pre-exponential factor calculated for each component of ficus nitida wood (hemicellulose, cellulose and lignin) according to the Friedman, Flynn-Wall-Ozawa and Vyazovkin methods. The dependence of E_a with the degree of conversion are shown in Figs. 3d, 4d and 5d. The results from Friedman, Flynn-Wall-Ozawa and Vyazovkin methods are similar to each other, making these results comparable among different methods. The three activation energy curves display a similar change, an increasing tendency with the increase of the conversion degree. These are in accord with reported findings by J. Nisar et al.[44–46]. Furthermore, it should be notice that the values from Flynn-Wall-Ozawa and Vyazovkin methods are slightly lower than those from the Fridman method. It is easy to explain the reason for the difference by analysing the calculation principles of the three methods. Flynn-Wall-Ozawa and Vyazovkin methods include some assumptions and approximations, but Friedman method not. The activation energy was determined to be 180.30 kJ/mol, 214.42 kJ/mol, and 248.23 kJ/mol from Friedman method; 172.31 kJ/mol, 206.48 kJ/mol, and 237.85 kJ/mol from FWO method; 171.40 kJ mol, 209.45 kJ/mol, and 239.05 kJ/mol from Vyavozkin method for decomposition of hemicellulose, cellulose and lignin respectively. In this sens, the distribution of activation

energies during the pyrolysis process of ficus wood was performed according to the conversion range. In stage I, x = 0.05-0.35, the values of activation energy of the hemicellulose decomposition were found to be 171.4-180.3 kJ.mol^{-1}. In stage II, x = 0.35-0.70, The cellulose decomposition generally took place in this pyrolysis stage. The values of activation energy are 206.48 kJ.mol^{-1} to 214.42 kJ.mol^{-1}. For stage III, x = 0.7-0.90, the calculated value of activation energy from the thermal decomposition of lignin varied within 237.85-248.23 kJ.mol^{-1}. It is noted that the activation energies follow the order of E_a (lignin) > E_a (cellulose) > E_a (hemicellulose), which indicates that the activation energy for the decomposition of lignin is the highest one then that of cellulose and hemicellulose. The order of E_a is in good agreement with the results reported by other autors [42,47–49]. Cai et al. [48] found an average value of Ea 169.7-186.8 kJ.mol^{-1}, 204.2-212.5 kJ.mol^{-1} and 237-266.6 kJ.mol^{-1} for hemicellulose, cellulose and lignin, respectively. Chen et al. [42] obtained activation energies of 148.12-164.56 kJ.mol^{-1}, 171.04-179.54 kJ.mol^{-1} and 175.71-201.6 for hemicellulose, cellulose and lignin, respectively. According to Anca-couce et al., [47] the activation energy was determined to be 150.8-179.3 kJ.mol^{-1}, 177.4-190.2 kJ.mol^{-1} and 203-211.4 kJ.mol^{-1} for hemicellulose, cellulose and lignin from beech wood, respectively. Hu et al. [49] determineted the mean activation energies for hemicelluloses, cellulose and lignin are 154.55-168.63 kJ.mol^{-1}, 188.14-206.71 kJ.mol^{-1} and 199.08-221.21 kJ.mol^{-1}, with standard deviations of 26.45-28.47, 23.79-24.88 and 33.31-37.24 kJ.mol^{-1}, respectively.

3.4. Reaction mechanisms by master-plots

In order for the complete reaction kinetics to be understood, the kinetic model need to be estimated. The kinetic models can be found using the integral master-plots when E is specified. The theoretical versus experimental master-plots are compared to obtain the most probable model. Based on the E_a value obtained using the FWO method, and the temperature

measured as a function of x, the experimental master-plots $\dfrac{P(u)}{P(u_{0,5})} = \dfrac{T^2}{T^2{}_{0,5}} \dfrac{exp(-E/RT)}{exp(-E/RT_{0,5})}$

can be determineted. The comparison of the theoretical masterplots with the experimental masterplots for decomposition of hemicellulose, cellulose and lignin is shown in Figs. 6, 7 and 8, respectively.

As shown in Figs. 6, 7 and 8, the experimental masterplots of $\dfrac{P(u)}{P(u_{0,5})}$ versus x at different heating rates are practically identical, indicating that the kinetics of hemicellulose, cellulose and lignin pyrolysis could be described by a single kinetic model. The comparison of the experimental masterplots with the theoretical ones in Fig. 6 indicates that the kinetic process for the decomposition of hemicellulose can be described by the diffusion model, since the experimental master-plots overlap D_4 of the theoretical master-plots. Therefore, the experimental masterplots in Fig. 7 shows that for cellulose decomposition, they were close to overlap the D2 curve. However, the P (u) /P (u0.5) plots (Fig. 8) for lignin decomposition can be described the theoretical master-plots F3, thus indicating that the reaction-order model best described the kinetic process of lignin. The results indicate that the diffusion process is followed by the pyrolysis of the ficus wood, at conversion values up to 0.75. When the conversion value increased above 0.75, the shape of experimental curve tends to follow F3 mechanism.

3.5. Estimation of pre-exponential factor and thermodynamic parameter

The pre-exponential factors (A) were calculated by using Eq. 13. In this study, pre-exponential factor was calculated using activation energy derived from isoconversionnel methods and variation in pre-exponential values with conversion are presented in Fig. 9.

The average values of pre-exponential factor for three pseudo-components of ficus wood ranges from $7,5.10^7$ to $1,84.10^{12}$ s^{-1} ($A_{Hemicellulose} = 1,12.10^{12}$ s^{-1}), $9,97.10^{12}$ to $1,6.10^{15}$ s^{-1} ($A_{Cellulose} = 1,14.10^{14}$ s^{-1}) and $1,77.10^{10}$ to $3,49.10^{15}$ s^{-1} ($A_{Lignin} = 3,4.10^{14}$ s^{-1}), respectively. The variation of the pre-exponential factor values is due to the complex composition of the biomass and also to the complex thermal behavior of the biomass. It was also noted that the pre-exponential factor value is proportional to the activation energy. It is generally admitted that there will be a linear relationship between the activation energy and the pre-exponential factors which is the so-called "kinetic compensation effects", as follows [50,51]:

$$lnA = a + bE$$
$$a = \ln(k_{iso})$$
$$b = \frac{1}{RT_{iso}}$$

where a and b are constants. k_{iso} and T_{iso} denote the artificial isokinetic rate constant and the artificial isokinetic temperature, respectively.

Fig. 10 shows the average linear fit obtained by the compensation effect for each pseudo-component of ficus nitida wood. The isokinetic parameters determined for each pseudo-component at four heating rates are shown in Table 5. Fig. 10 indicates a satisfactory linear fit for all pseudo-components, with a high regression coefficient ($R^2 \geq 9919$), which demonstrates a great approximation with the A values calculated by the linear equation. It is observed that when the heating rate increases, the value of the pre-exponential factor increases as well. This is due to increase in collision intensity at high heating rate.

Based upon the obtained values of A, the average values of ΔH, ΔG, and ΔS at four heating rates versus x are determineted and presented in Figs. 11d, 12d and 13d. It is presented in Figs. 11a,b,c, 12a,b,c and 13a,b,c that the average values of ΔH, ΔG, and ΔS in the whole

pyrolysis process maintain at a constant value, which indicates that the heating rate has little influence on ΔH, ΔG, and ΔS.

The enthalpy (ΔH) is the amount energy exchanged during a chemical reaction. For pyrolysis, the enthalpy is the energy consumed to convert biomass into bio-char, bio-oil and bio-gas. The positive values of ΔH (170.17 kJ.mol^{-1} for hemicellulose, 205.08 kJ.mol^{-1} for cellulose and 235.95 kJ.mol^{-1} for lignin) indicate that the pyrolysis of ficus nitida wood is endothermic process in nitrogen. The difference between E-values and the ΔH value for the three pseudo-components of ficus wood is about $\approx$ 5 kJ.mol^{-1}. This little difference of energy reflects that the product generation is being favored owing to low potential energy[52].

Gibbs free energy (ΔG) represents the total increase in total energy of the reaction during the formation of the activated complex. As mentined in Figs. 11b, 12b and 13c, the ΔG values maintain at a constant value with the increase of x during the decomposition of hemicellulose, cellulose and lignin. The average ΔG values of pseudo-components of ficus wood was 172.43, 186.48 and 220.01 kJ.mol^{-1}, respectively. Moreover, the high Gibb's free energy value observed for ficus wood pyrolysis showed that it has the potential to be utilized as a substitute for bio-energy production.

ΔS represents the degree of disorder which relates to the formation of the activated complex species. Figs. 11c, 12c and 13c represent the negative and positive values of amount of entropy as a function of conversion degree. In table 6, it was observed that average ΔS of pseudo-components of ficus wood has negative (-4.08 J.mol^{-1}), positive (+30.68 J.mol^{-1}) and positive (+22.49 J.mol^{-1}) values, respectively. The ΔS value is negative, suggesting that the reaction system moves from a disordered state to an ordered state, which is of great importance to convert ficus wood into biofuels and chemical feedstocks. The low ΔS means

the material just passes through some physical and chemical changes, bringing it to state near to its thermodynamic equilibrium [53]. The negative and positive values suggest the complexity of the thermal decomposition of ficus wood into bio-oil, bio-gas and biochar which may be further characterized using GC-MS, H-RMN and FTIR based analyses of the volatiles.

4- Conclusions:

In this study, the bioenergy potentiel of ficus nitida wood was analyzed using thermogravimetric study. To provide guidance its conversion to fuels or chemical raw materials, the physicochemical characteristics, kinetic behavior, and thermodynamics parameters are investigated by a thermogravimetric analyzer under nitrogen atmosphere at different heating rates of 5, 10, 20 and 50 K.min^{-1}.

The pyrolysis of ficus nitida wood in the range of $0.05 < x < 0.9$ can be roughly divided into three stages. Kinetics analysis indicated that the average activation energies for the pyrolysis of hemicellulose, cellulose and lignin were 171.4-180.3 kJ.mol^{-1}, 206.48-214.42 kJ.mol^{-1} and

237.85-248.23 kJ.mol^{-1}, respectively. The most optimal kinetic models for the pyrolysis of three pseudo-components of ficus wood were D4, D2 and F3, respectively.

Each of the ΔH and ΔG values maintains at a positive constant, whereas ΔS value is negative in the range of 5-35% and positive in two range 35-75% and 75-90%. In addition, the heating rate has little influence on the average values of ΔH, ΔG, and ΔS in the whole pyrolysis process.

In addition, the little difference in energy (≈ 5 kJ.mol^{-1}) between E and ΔH, which confirms that product formation requires only a low potential energy. From these parameters, it is concluded that the ficus wood has significant potential to be used as a feedstock for bioenergy/biofuels production.

References

[1]   Meyer PA, Snowden-Swan LJ, Jones SB, Rappé KG, Hartley DS. The effect of feedstock composition on fast pyrolysis and upgrading to transportation fuels: Techno-economic analysis and greenhouse gas life cycle analysis. Fuel 2020;259:116218. https://doi.org/10.1016/j.fuel.2019.116218.

[2]   Ubando AT, Rivera DRT, Chen W-H, Culaba AB. A comprehensive review of life cycle assessment (LCA) of microalgal and lignocellulosic bioenergy products from

thermochemical processes. Bioresource Technology 2019;291:121837. https://doi.org/10.1016/j.biortech.2019.121837.

[3] Amaniampong PN, Asiedu NY, Fletcher E, Dodoo-Arhin D, Olatunji OJ, Trinh QT. Conversion of Lignocellulosic Biomass to Fuels and Value-Added Chemicals Using Emerging Technologies and State-of-the-Art Density Functional Theory Simulations Approach. In: Daramola MO, Ayeni AO, editors. Valorization of Biomass to Value-Added Commodities: Current Trends, Challenges, and Future Prospects, Cham: Springer International Publishing; 2020, p. 193–220. https://doi.org/10.1007/978-3-030-38032-8_10.

[4] Arun N, Dalai AK. Chapter 9 - Environmental and socioeconomic impact assessment of biofuels from lignocellulosic biomass. In: Yousuf A, Pirozzi D, Sannino F, editors. Lignocellulosic Biomass to Liquid Biofuels, Academic Press; 2020, p. 283–99. https://doi.org/10.1016/B978-0-12-815936-1.00009-5.

[5] Moorman CE, Grodsky SM, Rupp S. Renewable Energy and Wildlife Conservation. JHU Press; 2019.

[6] Zucaro A, Fierro A, Forte A. A Review on Potential Candidate Lignocellulosic Feedstocks for Bio-energy Supply Chain. In: Basosi R, Cellura M, Longo S, Parisi ML, editors. Life Cycle Assessment of Energy Systems and Sustainable Energy Technologies: The Italian Experience, Cham: Springer International Publishing; 2019, p. 119–38. https://doi.org/10.1007/978-3-319-93740-3_8.

[7] Tursi A. A review on biomass: importance, chemistry, classification, and conversion. Biofuel Research Journal 2019;6:962–79. https://doi.org/10.18331/BRJ2019.6.2.3.

[8] Wei H, Liu W, Chen X, Yang Q, Li J, Chen H. Renewable bio-jet fuel production for aviation: A review. Fuel 2019;254:115599. https://doi.org/10.1016/j.fuel.2019.06.007.

[9] Pinho A de R, de Almeida MBB, Mendes FL, Casavechia LC, Talmadge MS, Kinchin CM, et al. Fast pyrolysis oil from pinewood chips co-processing with vacuum gas oil in

an FCC unit for second generation fuel production. Fuel 2017;188:462–73. https://doi.org/10.1016/j.fuel.2016.10.032.

[10] Moukrim S, Lahssini S, Naggar M, Lahlaoi H, Rifai N, Arahou M, et al. Local community involvement in forest rangeland management: case study of compensation on forest area closed to grazing in Morocco. Rangel J 2019;41:43–53. https://doi.org/10.1071/RJ17119.

[11] Šimelytė A. Chapter 13 - Promotion of renewable energy in Morocco. In: Tvaronavičienė M, Ślusarczyk B, editors. Energy Transformation Towards Sustainability, Elsevier; 2020, p. 249–87. https://doi.org/10.1016/B978-0-12-817688-7.00013-6.

[12] Zaher H, Sabir M, Benjelloun H, Paul-Igor H. Effect of forest land use change on carbohydrates, physical soil quality and carbon stocks in Moroccan cedar area. Journal of Environmental Management 2020;254:109544. https://doi.org/10.1016/j.jenvman.2019.109544.

[13] Cho EJ, Trinh LTP, Song Y, Lee YG, Bae H-J. Bioconversion of biomass waste into high value chemicals. Bioresource Technology 2020;298:122386. https://doi.org/10.1016/j.biortech.2019.122386.

[14] Singhvi MS, Gokhale DV. Lignocellulosic biomass: Hurdles and challenges in its valorization. Appl Microbiol Biotechnol 2019;103:9305–20. https://doi.org/10.1007/s00253-019-10212-7.

[15] Varma AK, Thakur LS, Shankar R, Mondal P. Pyrolysis of wood sawdust: Effects of process parameters on products yield and characterization of products. Waste Management 2019;89:224–35. https://doi.org/10.1016/j.wasman.2019.04.016.

[16] Wang A, Austin D, Song H. Investigations of thermochemical upgrading of biomass and its model compounds: Opportunities for methane utilization. Fuel 2019;246:443–53. https://doi.org/10.1016/j.fuel.2019.03.015.

[17] Khiari B, Ghouma I, Ferjani AI, Azzaz AA, Jellali S, Limousy L, et al. Kenaf stems: Thermal characterization and conversion for biofuel and biochar production. Fuel 2020;262:116654. https://doi.org/10.1016/j.fuel.2019.116654.

[18] Aboulkas A, Hammani H, El Achaby M, Bilal E, Barakat A. Valorization of algal waste via pyrolysis in a fixed-bed reactor: Production and characterization of bio-oil and bio-char. Bioresource Technology 2017;243:400–408.

[19] Setter C, Silva FTM, Assis MR, Ataíde CH, Trugilho PF, Oliveira TJP. Slow pyrolysis of coffee husk briquettes: Characterization of the solid and liquid fractions. Fuel 2020;261:116420. https://doi.org/10.1016/j.fuel.2019.116420.

[20] Zhan H, Zhuang X, Song Y, Liu J, Li S, Chang G, et al. A review on evolution of nitrogen-containing species during selective pyrolysis of waste wood-based panels. Fuel 2019;253:1214–28. https://doi.org/10.1016/j.fuel.2019.05.122.

[21] Xiong Z, Wang Y, Syed-Hassan SSA, Hu X, Han H, Su S, et al. Effects of heating rate on the evolution of bio-oil during its pyrolysis. Energy Conversion and Management 2018;163:420–7. https://doi.org/10.1016/j.enconman.2018.02.078.

[22] Slopiecka K, Bartocci P, Fantozzi F. Thermogravimetric analysis and kinetic study of poplar wood pyrolysis. Applied Energy 2012;97:491–7. https://doi.org/10.1016/j.apenergy.2011.12.056.

[23] Sobek S, Werle S. Kinetic modelling of waste wood devolatilization during pyrolysis based on thermogravimetric data and solar pyrolysis reactor performance. Fuel 2020;261:116459. https://doi.org/10.1016/j.fuel.2019.116459.

[24] Singh S, Prasad Chakraborty J, Kumar Mondal M. Intrinsic kinetics, thermodynamic parameters and reaction mechanism of non-isothermal degradation of torrefied Acacia nilotica using isoconversional methods. Fuel 2020;259:116263. https://doi.org/10.1016/j.fuel.2019.116263.

[25] Zou H, Li W, Liu J, Buyukada M, Evrendilek F. Catalytic combustion performances, kinetics, reaction mechanisms and gas emissions of Lentinus edodes. Bioresource Technology 2020;300:122630. https://doi.org/10.1016/j.biortech.2019.122630.

[26] Zou H, Zhang J, Liu J, Buyukada M, Evrendilek F, Liang G. Pyrolytic behaviors, kinetics, decomposition mechanisms, product distributions and joint optimization of Lentinus edodes stipe. Energy Conversion and Management 2020;213:112858. https://doi.org/10.1016/j.enconman.2020.112858.

[27] Cai H, Liu J, Xie W, Kuo J, Buyukada M, Evrendilek F. Pyrolytic kinetics, reaction mechanisms and products of waste tea via TG-FTIR and Py-GC/MS. Energy Conversion and Management 2019;184:436–47. https://doi.org/10.1016/j.enconman.2019.01.031.

[28] Grønli MG, Várhegyi G, Di Blasi C. Thermogravimetric analysis and devolatilization kinetics of wood. Industrial & Engineering Chemistry Research 2002;41:4201–4208.

[29] Mishra G, Kumar J, Bhaskar T. Kinetic studies on the pyrolysis of pinewood. Bioresource Technology 2015;182:282–8. https://doi.org/10.1016/j.biortech.2015.01.087.

[30] Poletto M. Thermogravimetric analysis and kinetic study of pine wood pyrolysis. Revista Ciência Da Madeira (Brazilian Journal of Wood Science) 2016;7. https://doi.org/10.15210/cmad.v7i2.7383.

[31] Xu X, Chen R, Pan R, Zhang D. Pyrolysis Kinetics, Thermodynamics, and Volatiles of Representative Pine Wood with Thermogravimetry–Fourier Transform Infrared Analysis. Energy Fuels 2020;34:1859–69. https://doi.org/10.1021/acs.energyfuels.9b03872.

[32] He Q, Ding L, Gong Y, Li W, Wei J, Yu G. Effect of torrefaction on pinewood pyrolysis kinetics and thermal behavior using thermogravimetric analysis. Bioresource Technology 2019;280:104–11. https://doi.org/10.1016/j.biortech.2019.01.138.

[33] Friedman HL. Kinetics of thermal degradation of char-forming plastics from thermogravimetry. Application to a phenolic plastic. J Polym Sci, C Polym Symp 1964;6:183–95. https://doi.org/10.1002/polc.5070060121.

[34] Flynn JH, Wall LA. General treatment of the thermogravimetry of polymers. J Res Nat Bur Stand 1966;70:487–523.

[35] Flynn JH, Wall LA. A quick, direct method for the determination of activation energy from thermogravimetric data. J Polym Sci B Polym Lett 1966;4:323–8. https://doi.org/10.1002/pol.1966.110040504.

[36] Ozawa T. A New Method of Analyzing Thermogravimetric Data. BCSJ 1965;38:1881–6. https://doi.org/10.1246/bcsj.38.1881.

[37] Doyle CD. Kinetic analysis of thermogravimetric data. J Appl Polym Sci 1961;5:285–92. https://doi.org/10.1002/app.1961.070051506.

[38] Sbirrazzuoli N. Determination of pre-exponential factors and of the mathematical functions f(α) or G(α) that describe the reaction mechanism in a model-free way. Thermochimica Acta 2013;564:59–69. https://doi.org/10.1016/j.tca.2013.04.015.

[39] Vyazovkin S, Sbirrazzuoli N. Confidence intervals for the activation energy estimated by few experiments. Analytica Chimica Acta 1997;355:175–80. https://doi.org/10.1016/S0003-2670(97)00505-9.

[40] Doyle CD. Series Approximations to the Equation of Thermogravimetric Data. Nature 1965;207:290–1. https://doi.org/10.1038/207290a0.

[41] Yuan X, He T, Cao H, Yuan Q. Cattle manure pyrolysis process: Kinetic and thermodynamic analysis with isoconversional methods. Renewable Energy 2017;107:489–96. https://doi.org/10.1016/j.renene.2017.02.026.

[42] Chen Z, Hu M, Zhu X, Guo D, Liu S, Hu Z, et al. Characteristics and kinetic study on pyrolysis of five lignocellulosic biomass via thermogravimetric analysis. Bioresource Technology 2015;192:441–50. https://doi.org/10.1016/j.biortech.2015.05.062.

[43] Kaur R, Gera P, Jha MK, Bhaskar T. Pyrolysis kinetics and thermodynamic parameters of castor (Ricinus communis) residue using thermogravimetric analysis. Bioresource Technology 2018;250:422–8. https://doi.org/10.1016/j.biortech.2017.11.077.

[44] Nisar J, Rahman A, Ali G, Shah A, Farooqi ZH, Bhatti IA, et al. Pyrolysis of almond shells waste: effect of zinc oxide on kinetics and product distribution. Biomass Conv Bioref 2020. https://doi.org/10.1007/s13399-020-00762-6.

[45] Nisar J, Ali G, Shah A, Iqbal M, Khan RA, Sirajuddin, et al. Fuel production from waste polystyrene via pyrolysis: Kinetics and products distribution. Waste Management 2019;88:236–47. https://doi.org/10.1016/j.wasman.2019.03.035.

[46] Nisar J, Ali F, Malana MA, Ali G, Iqbal M, Shah A, et al. Kinetics of the pyrolysis of cobalt-impregnated sesame stalk biomass. Biomass Conv Bioref 2019. https://doi.org/10.1007/s13399-019-00477-3.

[47] Anca-Couce A, Berger A, Zobel N. How to determine consistent biomass pyrolysis kinetics in a parallel reaction scheme. Fuel 2014;123:230–40. https://doi.org/10.1016/j.fuel.2014.01.014.

[48] Cai J, Wu W, Liu R, Huber GW. A distributed activation energy model for the pyrolysis of lignocellulosic biomass. Green Chem 2013;15:1331–40. https://doi.org/10.1039/C3GC36958G.

[49] Hu M, Chen Z, Wang S, Guo D, Ma C, Zhou Y, et al. Thermogravimetric kinetics of lignocellulosic biomass slow pyrolysis using distributed activation energy model, Fraser–Suzuki deconvolution, and iso-conversional method. Energy Conversion and Management 2016;118:1–11. https://doi.org/10.1016/j.enconman.2016.03.058.

[50] Nisar J, Khan MA, Ali G, Iqbal M, Shah A, Shah MR, et al. Pyrolysis of polypropylene over zeolite mordenite ammonium: kinetics and products distribution. Journal of Polymer Engineering 2019;39:785–93. https://doi.org/10.1515/polyeng-2019-0077.

[51] Ali G, Nisar J, Iqbal M, Shah A, Abbas M, Shah MR, et al. Thermo-catalytic decomposition of polystyrene waste: Comparative analysis using different kinetic models: Waste Management & Research 2019. https://doi.org/10.1177/0734242X19865339.

[52] Nisar J, Ali G, Shah A, Shah MR, Iqbal M, Ashiq MN, et al. Pyrolysis of Expanded Waste Polystyrene: Influence of Nickel-Doped Copper Oxide on Kinetics, Thermodynamics, and Product Distribution. Energy Fuels 2019;33:12666–78. https://doi.org/10.1021/acs.energyfuels.9b03004.

[53] Huang L, Liu J, He Y, Sun S, Chen J, Sun J, et al. Thermodynamics and kinetics parameters of co-combustion between sewage sludge and water hyacinth in CO2/O2 atmosphere as biomass to solid biofuel. Bioresource Technology 2016;218:631–42. https://doi.org/10.1016/j.biortech.2016.06.133.

Figure captions

Fig. 1: Conversion x and its derivative (dx/dt) curves of ficus nitida wood at heating rate 5, 10, 20 and 50 K.min^{-1}

Fig. 2: Characteristic of temperature of pseudo-components of ficus wood by using second derivative method.

Fig. 3: Linear plots for determining activation energy of hemicellulose calculated by FR (a), FWO (b) and VYA (c); (d) the dependence of activation energy with the degree of conversion

Fig. 4: Linear plots for determining activation energy of cellulose calculated by FR (a), FWO (b) and VYA (c); (d) the dependence of activation energy with the degree of conversion

Fig. 5: Linear plots for determining activation energy of lignin calculated by FR (a), FWO (b) and VYA (c); (d) the dependence of activation energy with the degree of conversion

Fig. 6: Master plots of theoretical g(x)/g(0.5) and experimental master plots for the decomposition of Hemicellulose at a heating rates of 5, 10, 20 and 50 K.min^{-1}.

Fig. 7: Master plots of theoretical g(x)/g(0.5) and experimental master plots for the decomposition of Cellulose at a heating rates of 5, 10, 20 and 50 K.min^{-1}.

Fig. 8: Master plots of theoretical g(x)/g(0.5) and experimental master plots for the decomposition of Lignin at a heating rates of 5, 10, 20 and 50 K.min^{-1}.

Fig. 9: Pre-exponential factor at different conversion degree for three pseudo-components of ficus wood: (a)-Hemicellulose, (b)-Cellulose and (c)-Lignin.

Fig. 10: Isokinetic relationships between ln A and E for three pseudo-components of ficus wood at four heating rates: (a)-Hemicellulose, (b)-Cellulose and (c)-Lignin.

Fig. 11: (a) ΔH, (b) ΔG and (c) ΔS at different conversion degree; (d) ΔH, ΔG and ΔS at heating rates of 5, 10, 20 and 50 K.min^{-1} for hemicellulose.

Fig. 12: (a) ΔH, (b) ΔG and (c) ΔS at different conversion degree; (d) ΔH, ΔG and ΔS at heating rates of 5, 10, 20 and 50 K.min^{-1} for Cellulose.

Fig. 13: (a) ΔH, (b) ΔG and (c) ΔS at different conversion degree; (d) ΔH, ΔG and ΔS at heating rates of 5, 10, 20 and 50 K.min^{-1} for Lignin.

Tables list

Table 1: Proximate and elemental analyses of ficus nitida wood

Figure 1

Figure 2

Figure 3

Figure 4
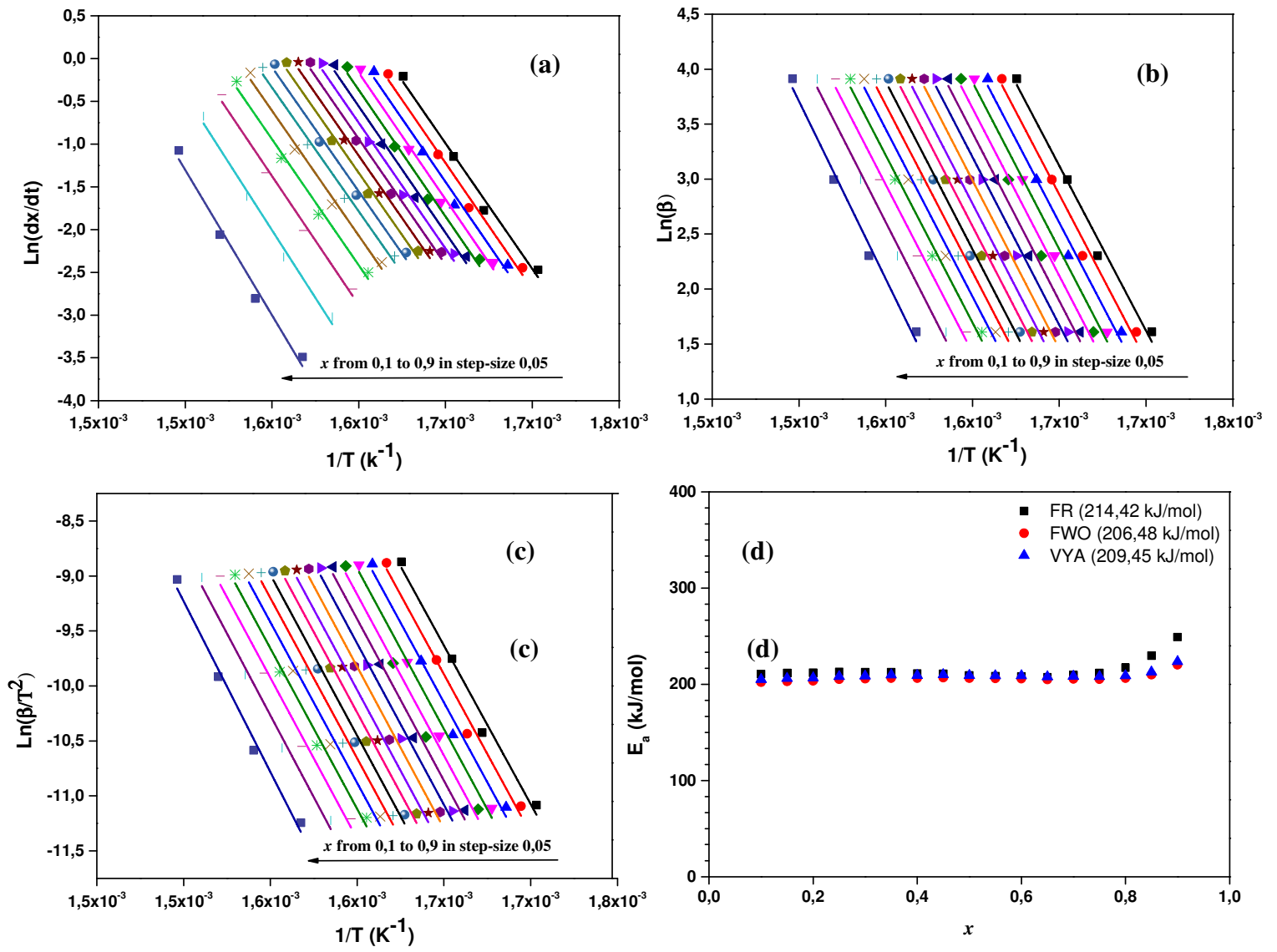
Figure 5
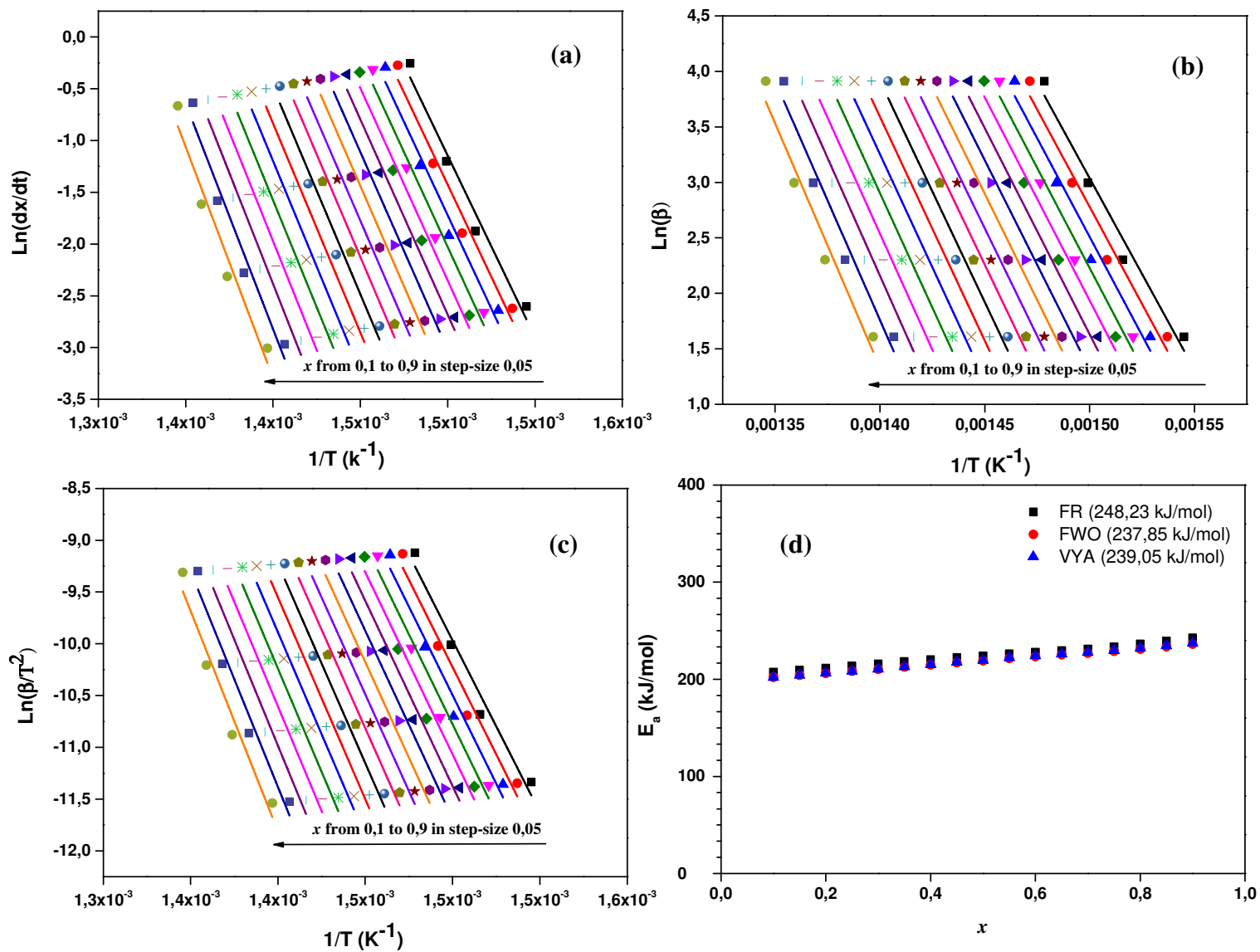
Figure 6
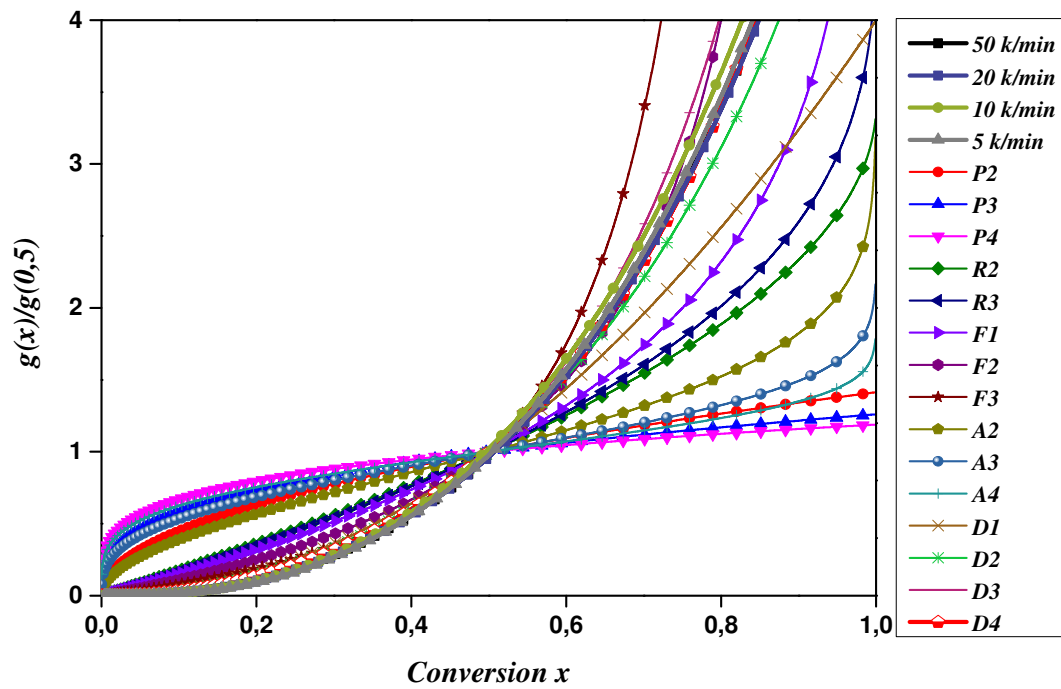
Figure 7
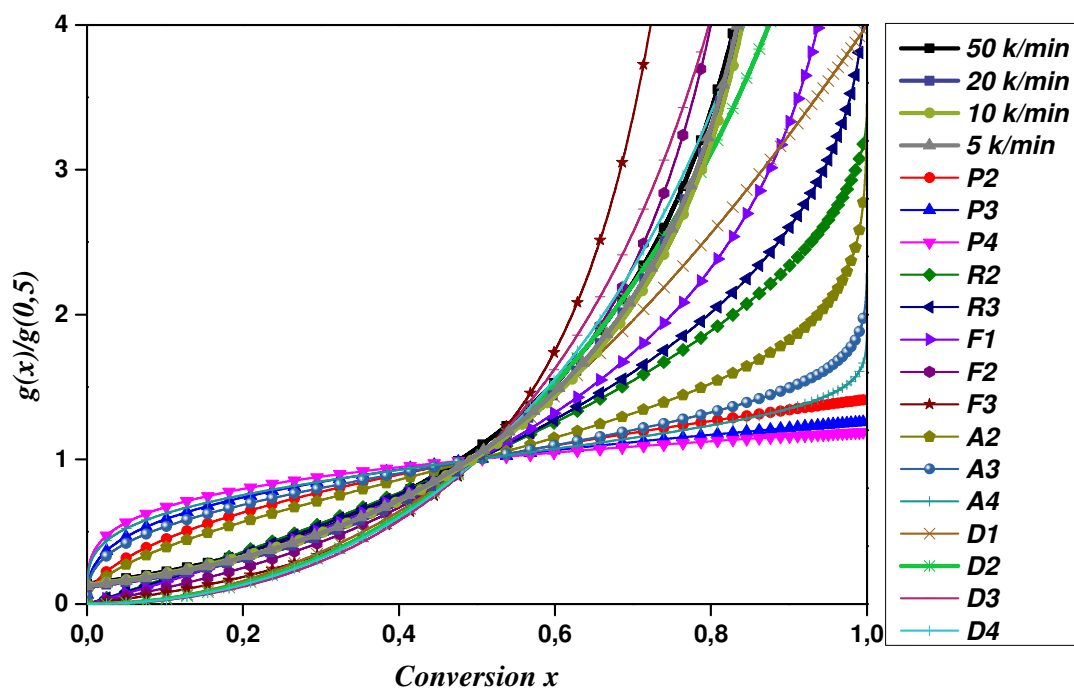
Figure 8
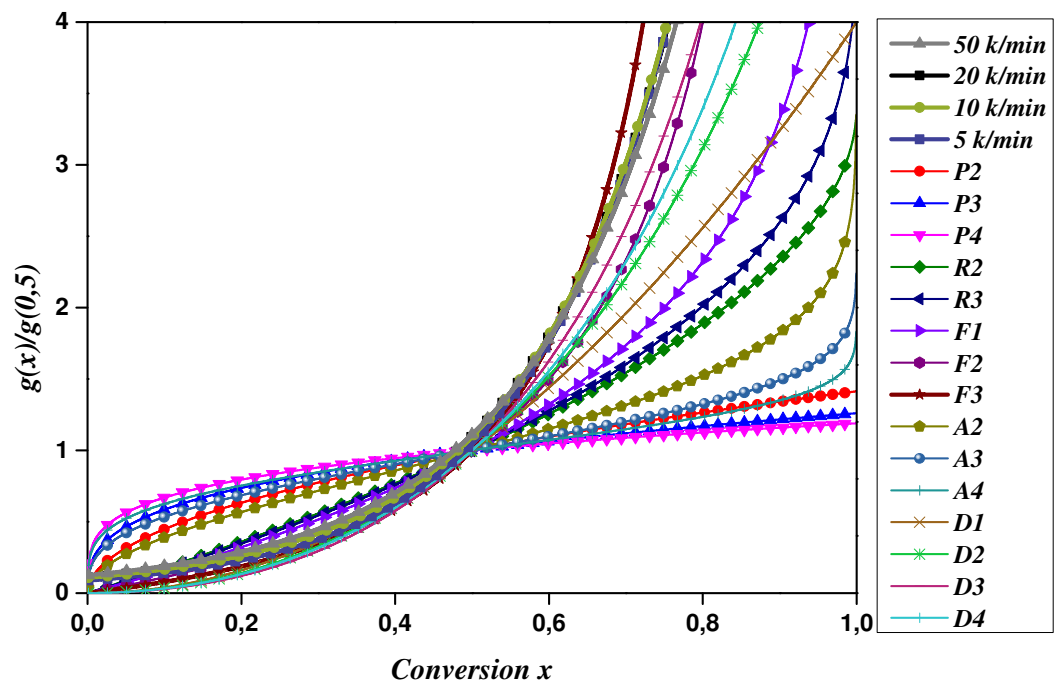
Figure 9
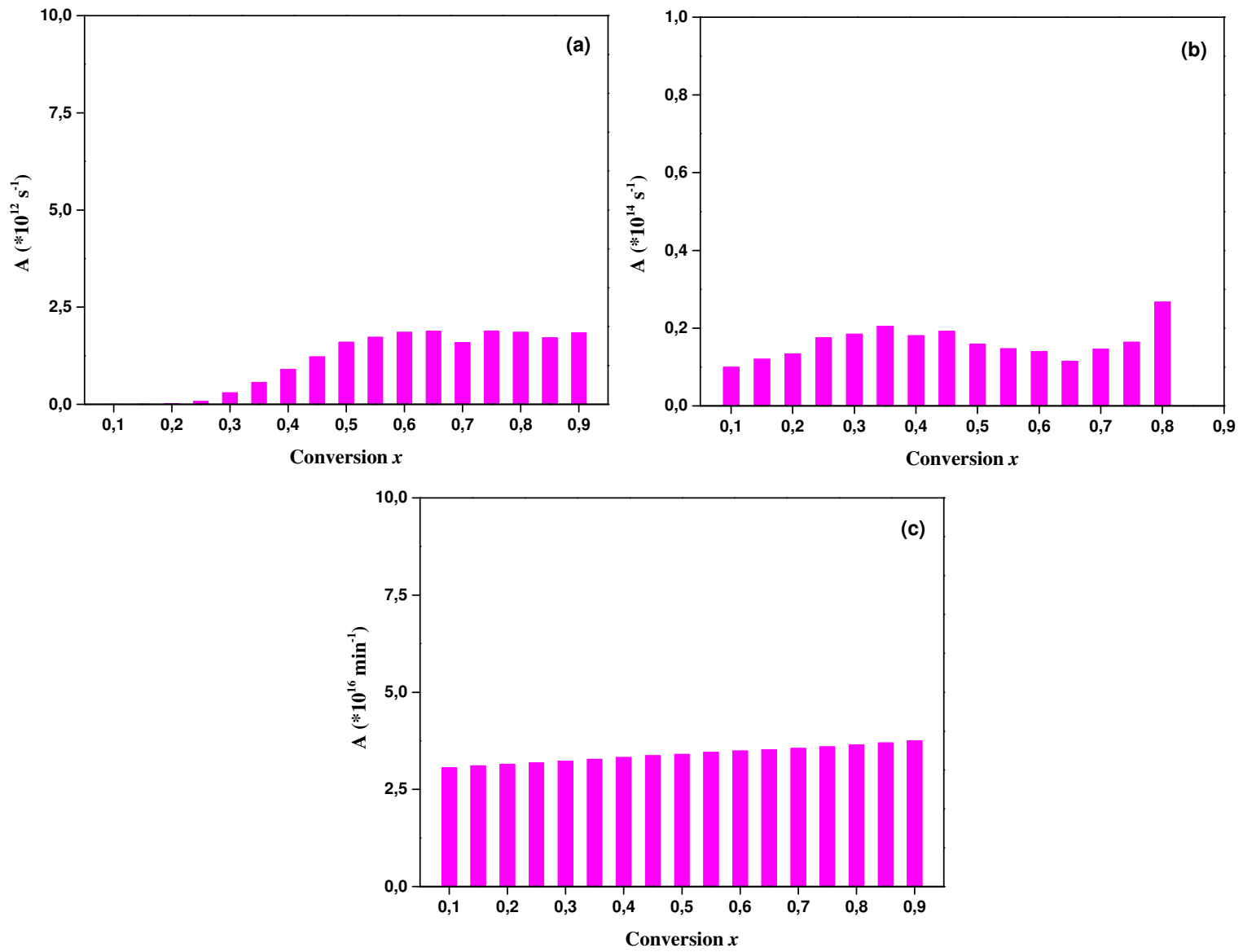
Figure 10
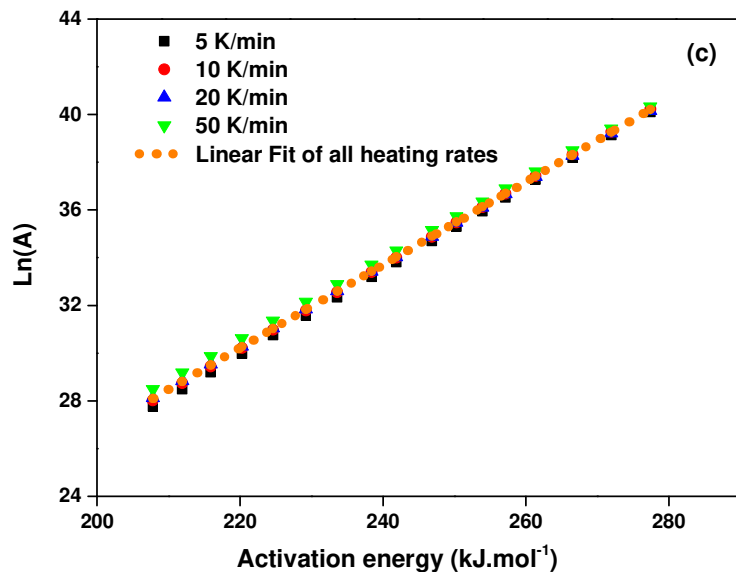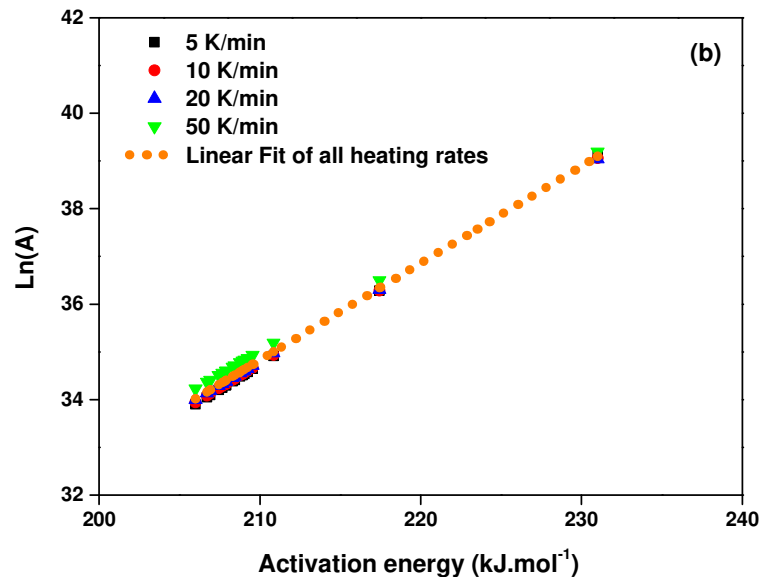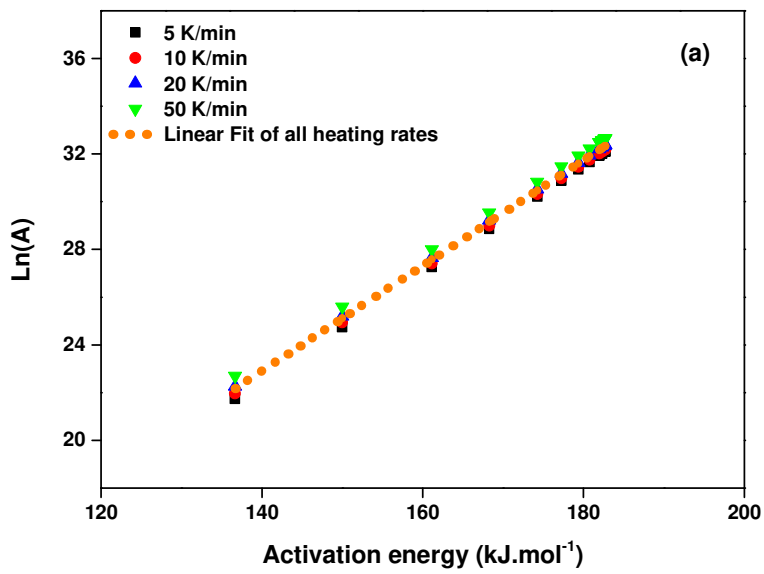
Figure 11
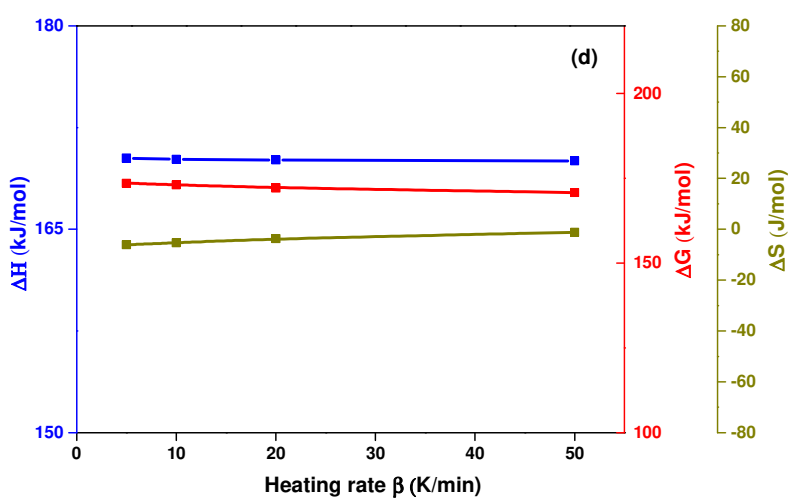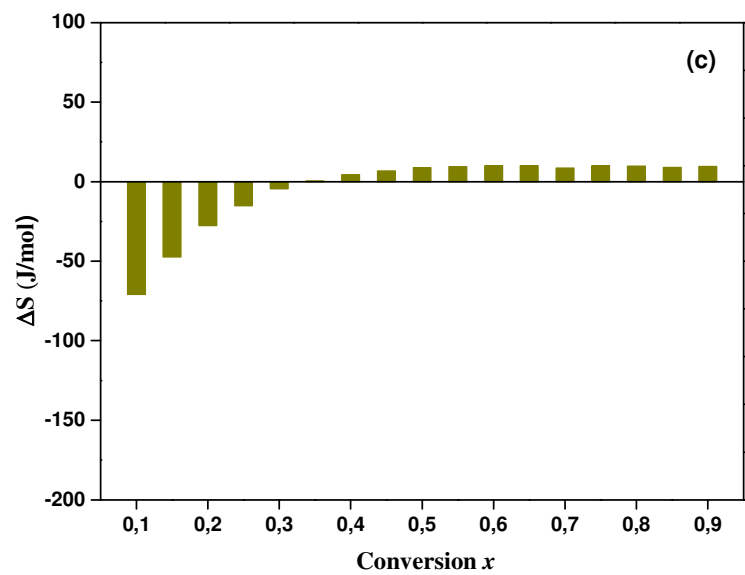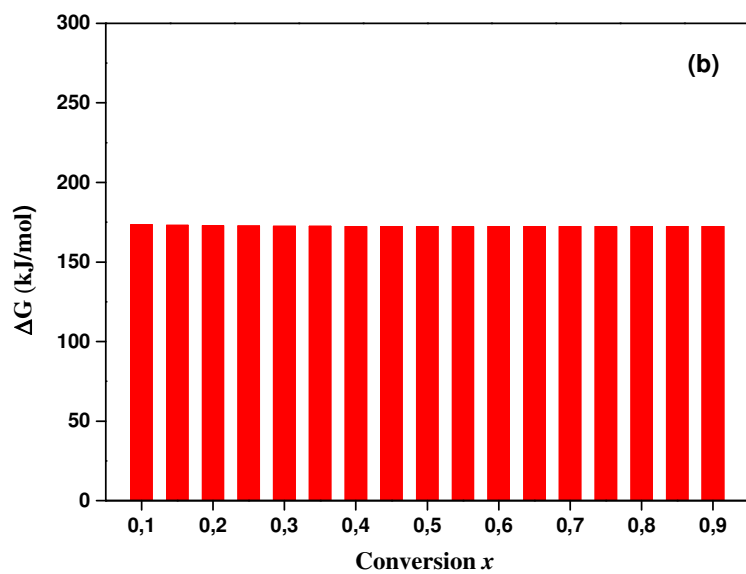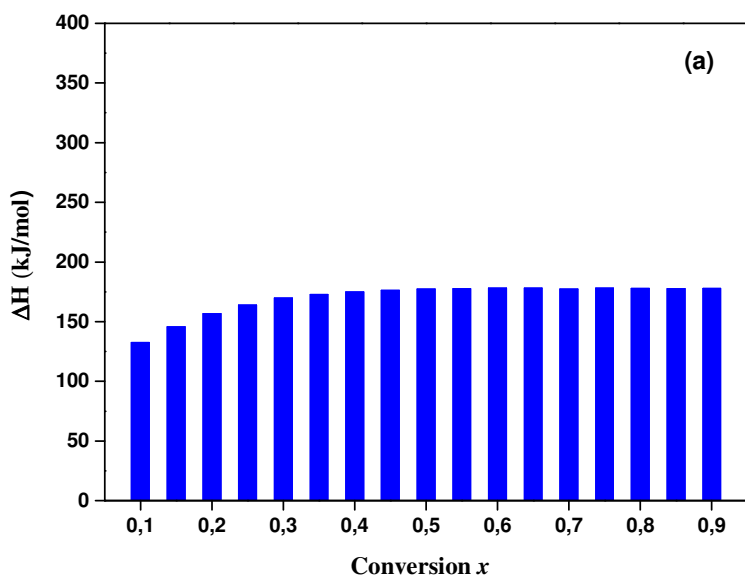
Figure 12
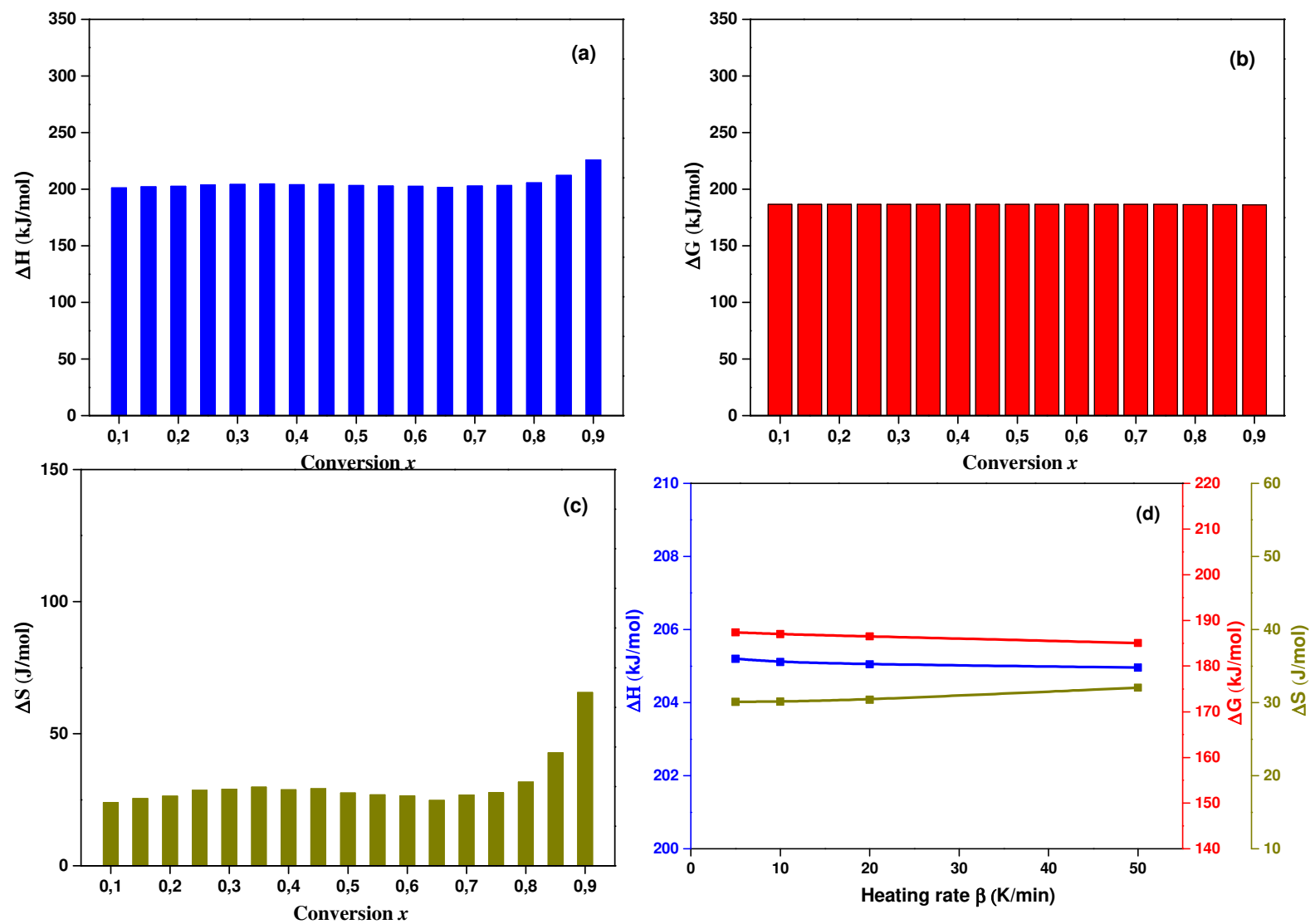
Figure 13
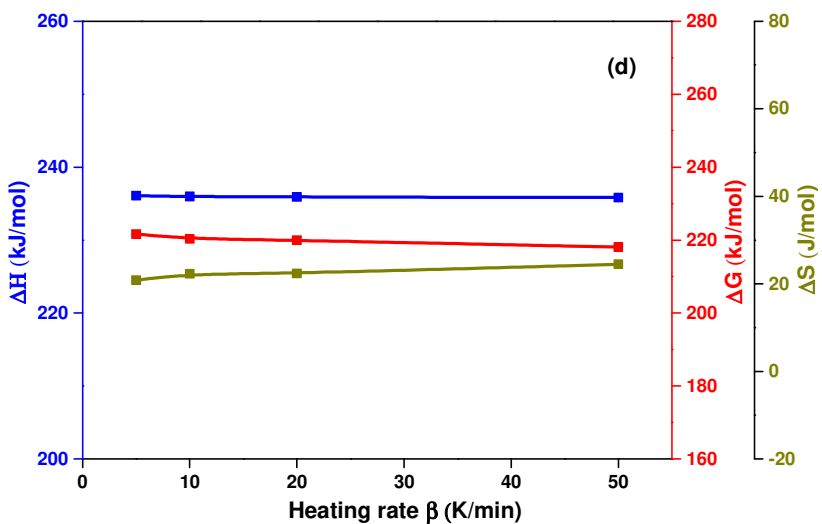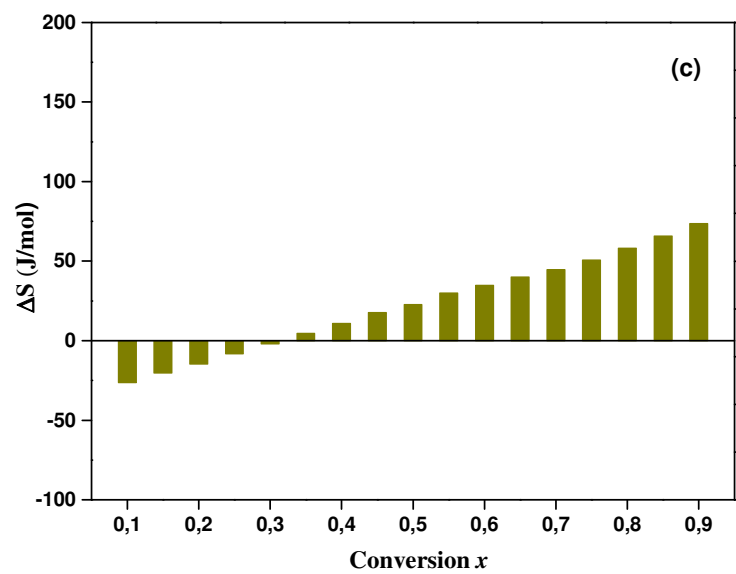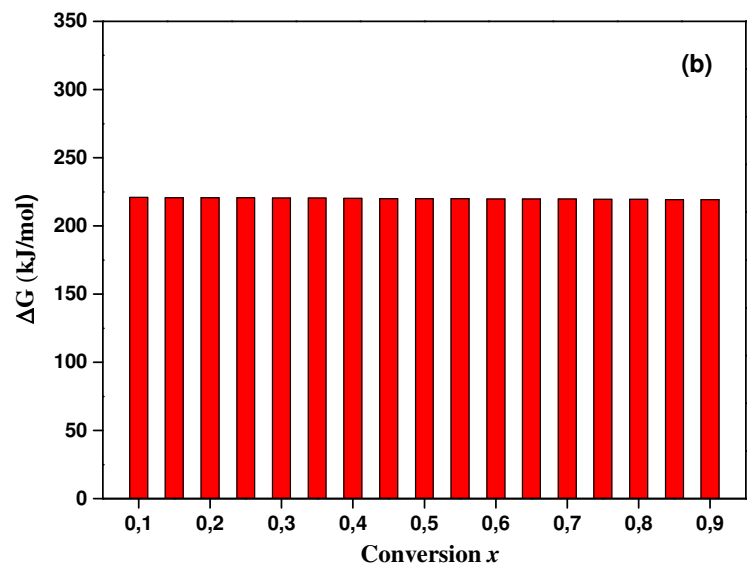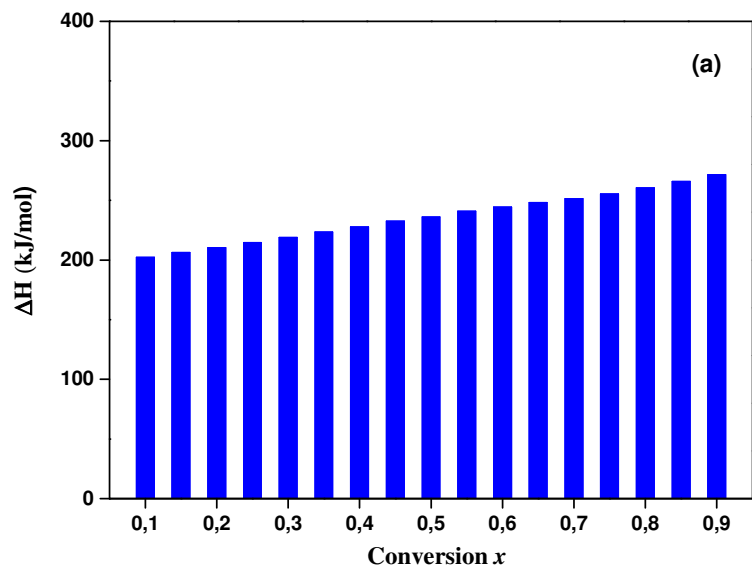
Table 1

Characteristics		Percentage
Proximate analysis (wt. %)	Moisture content	5.38
	Volatile matter	68.75
	Ash	14.4
	Fixed carbon	16.85
Ultimate analysis (wt. %)	Carbon	43.55
	Hydrogen	5.76
	Nitrogen	0.68
	Sulfur	--
	Oxygen	38.61
Fiber analysis (wt. %)	Extractive	5.33
	Hemicellulose	31.78
	Cellulose	41.09
	Lignin	21.80
H/C molar ratio		1.587
O/C molar ratio		0.665
Empirical formula		$CH_{1.587}O_{0.667}N_{0.013}$
Higher heating value (MJ kg^{-1})		16.82

Table 2

Model		Differentialform $f(x) = \dfrac{1}{k}\dfrac{dx}{dt}$	Integralform $g(x)$
		Nucleation models	
Power law	**P2**	$2x^{1/2}$	$x^{1/2}$
Power law	**P3**	$3x^{2/3}$	$x^{1/3}$
Power law	**P4**	$4x^{3/4}$	$x^{1/4}$
Avarami-Erofeyev	**A2**	$2(1-x)[-\ln(1-x)]^{1/2}$	$[-\ln(1-x)]^{1/2}$
Avarami-Erofeyev	**A3**	$3(1-x)[-\ln(1-x)]^{2/3}$	$[-\ln(1-x)]^{1/3}$
Avarami-Erofeyev	**A4**	$4(1-x)[-\ln(1-x)]^{3/4}$	$[-\ln(1-x)]^{1/4}$
		Geometrical contraction models	
Contracting area	**R2**	$2(1-x)^{1/2}$	$[1-(1-x)^{1/2}]$
Contracting volume	**R3**	$3(1-x)^{2/3}$	$[1-(1-x)^{1/3}]$
		Diffusion models	
1-D diffusion	**D1**	$1/2x$	x^2
2-D diffusion	**D2**	$[-\ln(1-x)]^{-1}$	$[(1-x)\ln(1-x)]+x$
3-D diffusion, Jander	**D3**	$3(1-x)^{2/3}/[2(1-(1-x)^{1/3})]$	$[1-(1-x)^{1/3}]^2$
Ginstling-Brounshtein	**D4**	$3/[2((1-x)^{-1/3}-1)]$	$1-(2x/3)-(1-x)^{2/3}$
		Reaction-order models	
First-order	**F1**	$(1-x)$	$-\ln(1-x)$
Second-order	**F2**	$(1-x)^2$	$(1-x)^{-1}-1$
Third-order	**F3**	$(1-x)^3$	$[(1-x)^{-2}-1]/2$

Table 3

	Stage I			Stage II			Stage III		
	$T_i(°C)$	$T_m(°C)$	$T_f(°C)$	$T_i(°C)$	$T_m(°C)$	$T_f(°C)$	$T_i(°C)$	$T_m(°C)$	$T_f(°C)$
5 K.min^{-1}	171	276	291	291	319	367	367	421	447
10 K.min^{-1}	180	284	301	301	328	380	380	429	460
20 K.min^{-1}	193	291	307	307	337	387	387	440	468
50 K.min^{-1}	206	300	317	317	347	397	397	451	475

Table 4

Isoconversional methods	E_a, kJ/mol Friedman	E_a, kJ/mol Flynn-Wall-Ozawa	E_a, kJ/mol Vyazovkin
Hemicellulose	180,30±7	172,31±3	171,40±3
cellulose	214,42±11	206,48±3	209,45±3
lignin	248.23±9	237.85±5	239.05±6

Table 5

	Hemicellulose				Cellulose				Lignin			
	a	b	K_{iso}	T_{iso}	a	b	K_{iso}	T_{iso}	a	b	K_{iso}	T_{iso}
5 K/min	-9,0439	0,2253	0,00012	533,96	-8,8914	0,2078	0,00014	578,93	-9,1134	0,1775	0,00011	677,74
10 K/min	-8,3797	0,2221	0,00023	541,50	-8,2285	0,2047	0,00027	587,53	-8,4432	0,1755	0,00022	685,39
20 K/min	-7,7115	0,2194	0,00045	548,12	-7,5651	0,2018	0,00052	596,15	-7,7812	0,1729	0,00042	695,86
50 K/min	-6,8269	0,2161	0,00108	556,62	-6,6013	0,1986	0,00136	605,70	-6,8955	0,1703	0,00101	706,36

Table 6

	Hemicellulose				Cellulose				Lignin			
	A min^{-1}	ΔH kJ/mol	ΔG kJ/mol	ΔS J/mol	A min^{-1}	ΔH kJ/mol	ΔG kJ/mol	ΔS J/mol	A min^{-1}	ΔH kJ/mol	ΔG kJ/mol	ΔS J/mol
5 K/min	$5{,}23.10^{13}$	170.24	173.59	-6.11	$6{,}74.10^{15}$	205.20	187.38	30.1	$2{,}54.10^{16}$	236,08	221,63	20,82
10 K/min	$5{,}73.10^{13}$	170.16	173.11	-5.30	$6{,}54.10^{15}$	205.11	186.99	30.15	$2{,}9.10^{16}$	235,98	220,34	22,28
20 K/min	$6{,}87.10^{13}$	170.11	172.21	-3.72	$6{,}49.10^{15}$	205.05	186.50	30.4	$2{,}72.10^{16}$	235,91	219,96	22,38
50 K/min	$9{,}05.10^{13}$	170.04	170.82	-1.19	$7{,}62.10^{15}$	204.96	185.05	32.06	$3{,}28.10^{16}$	235,84	218,11	24,49
Average value	**$6{,}72.10^{13}$**	**170,14**	**172,43**	**-4,08**	**$6{,}85.10^{15}$**	**205,08**	**186,48**	**30,68**	**$2{,}86.10^{16}$**	**235,95**	**220,01**	**22,49**
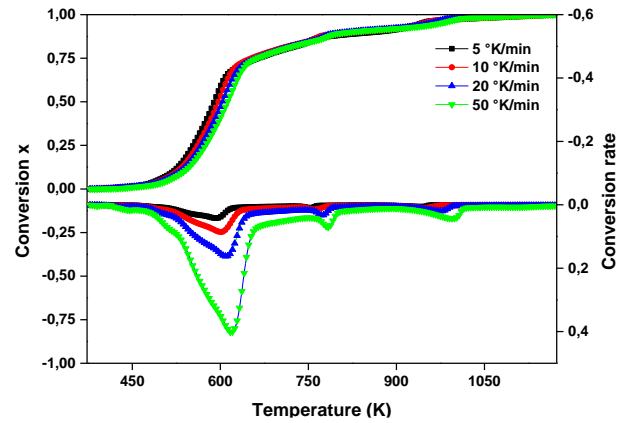
Thermal Behavior
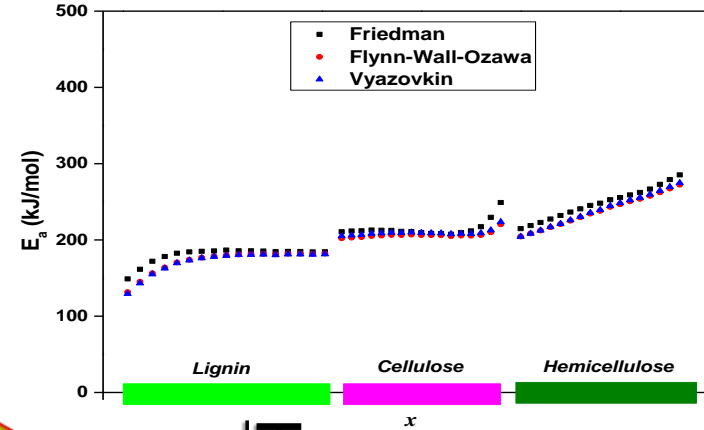
Kinetic Behavior

Thermodynamic Behavior

Pyrolysis by TGA

Ficus nitida wood

$105 \leq T(°C) \leq 900$

$5 \leq \beta(°C/min) \leq 50$

Friedman
Flynn-Wall-Ozawa
Vyazovkin

E_a (kJ/mol)

Lignin

Cellulose

Hemicellulose

x

Conversion x

Conversion rate

Temperature (K)

5 °K/min
10 °K/min
20 °K/min
50 °K/min

ΔH (kJ/mol)

ΔG (kJ/mol)

ΔS (J/mol)

Heating rate β (K/min)

(d)

$g(x)/g(0,5)$

Hemicellulose

Conversion x

50 k/min
20 k/min
10 k/min
5 k/min
P2
P3
P4
R2
R3
F1
F2
F3
A2
A3
A4
D1
D2
D3
D4